AFRL-AFOSR-VA-TR-2015-0251

MULTICOLOR (UV-IR) PHOTODETECTORS BASED ON LATTICE MATCHED 6.1A II/IV AND III/V SEMICONDUCTORS

Yong-Hang Zhang
ARIZONA STATE UNIVERSITY

08/27/2015
Final Report

Air Force Research Laboratory
AF Office Of Scientific Research (AFOSR)/ RTD
Arlington, Virginia 22203
Air Force Materiel Command

REPORT DOCUMENTATION PAGE

Form Approved
OMB No. 0704-0188

1. REPORT DATE *(DD-MM-YYYY)*	2. REPORT TYPE	3. DATES COVERED *(From - To)*
11-08-2015	Final	01-04-2012 to 14-05-2015

4. TITLE AND SUBTITLE
Multicolor (UV-IR) Photodetectors Based on Lattic Matched 61A IIIV and IIIV Semiconductors

5a. CONTRACT NUMBER

5b. GRANT NUMBER
FA9550-10-1-0129

5c. PROGRAM ELEMENT NUMBER

6. AUTHOR(S)
Yong-Hang Zhang

5d. PROJECT NUMBER

5e. TASK NUMBER

5f. WORK UNIT NUMBER

7. PERFORMING ORGANIZATION NAME(S) AND ADDRESS(ES)
Arizona State University
Office for Research and Sponsored Projects
PO Box 876011
Tempe, AZ 85257-6011

8. PERFORMING ORGANIZATION REPORT NUMBER

9. SPONSORING/MONITORING AGENCY NAME(S) AND ADDRESS(ES)
AFOSR/PKS FA9550
USAF, AFRL, AF Office of Scientific Research
875 N. Randolph St. Room 3112
Arlington, VA 22203

10. SPONSOR/MONITOR'S ACRONYM(S)
AFOSR

11. SPONSOR/MONITOR'S REPORT NUMBER(S)

12. DISTRIBUTION/AVAILABILITY STATEMENT
Distribution A

13. SUPPLEMENTARY NOTES

14. ABSTRACT
This program focused on the demonstration of a novel idea to use optical biasing for multi-color detection using two-terminal monolithically integrated multi-junction photodetectors (MJPDs). Using optical biasing, any sub-photodetector can be selected to limit the current and the multi-color photodetector detects light within the wavelength range of the selected sub-photodetector, namely, optical addressing. This idea has been firstly demonstrated in a monolithic GaInP/Ga(In)As/Ge triple-junction solar cell. Later on, the optical addressing has been achieved in a near-and-long-wave infrared multiband photodetector integrated by a NIR AlGaAs/GaAs PIN sub-photodetector and a LWIR AlGaAs/GaAs n-QWIP sub-photodetector. Finally, the optical addressing has been realized in a visible-and-mid-wave-infrared multi-color photodetector based on II-VI and III-V semiconductors. This photodetector consists of a newly-proposed CdTe/ZnTe/CdTe nBn sub-photodetector for visible light detection and a well-developed InSb PIN sub-photodetector for MWIR detection, which are electrically connected by a perfectly conductive n-CdTe/p-InSb tunnel junction.

15. SUBJECT TERMS
optical biasing; multi-junction photodetectors; triple-junction solar cell; integrated photonic devices

16. SECURITY CLASSIFICATION OF:			17. LIMITATION OF ABSTRACT	18. NUMBER OF PAGES	19a. NAME OF RESPONSIBLE PERSON
a. REPORT	b. ABSTRACT	c. THIS PAGE			Yong-Hang Zhang
UU	UU	UU	UU	19	19b. TELEPHONE NUMBER *(Include area code)* 480-727-2795

INSTRUCTIONS FOR COMPLETING SF 298

1. REPORT DATE. Full publication date, including day, month, if available. Must cite at least the year and be Year 2000 compliant, e.g. 30-06-1998; xx-06-1998; xx-xx-1998.

2. REPORT TYPE. State the type of report, such as final, technical, interim, memorandum, master's thesis, progress, quarterly, research, special, group study, etc.

3. DATES COVERED. Indicate the time during which the work was performed and the report was written, e.g., Jun 1997 - Jun 1998; 1-10 Jun 1996; May - Nov 1998; Nov 1998.

4. TITLE. Enter title and subtitle with volume number and part number, if applicable. On classified documents, enter the title classification in parentheses.

5a. CONTRACT NUMBER. Enter all contract numbers as they appear in the report, e.g. F33615-86-C-5169.

5b. GRANT NUMBER. Enter all grant numbers as they appear in the report, e.g. AFOSR-82-1234.

5c. PROGRAM ELEMENT NUMBER. Enter all program element numbers as they appear in the report, e.g. 61101A.

5d. PROJECT NUMBER. Enter all project numbers as they appear in the report, e.g. 1F665702D1257; ILIR.

5e. TASK NUMBER. Enter all task numbers as they appear in the report, e.g. 05; RF0330201; T4112.

5f. WORK UNIT NUMBER. Enter all work unit numbers as they appear in the report, e.g. 001; AFAPL30480105.

6. AUTHOR(S). Enter name(s) of person(s) responsible for writing the report, performing the research, or credited with the content of the report. The form of entry is the last name, first name, middle initial, and additional qualifiers separated by commas, e.g. Smith, Richard, J, Jr.

7. PERFORMING ORGANIZATION NAME(S) AND ADDRESS(ES). Self-explanatory.

8. PERFORMING ORGANIZATION REPORT NUMBER. Enter all unique alphanumeric report numbers assigned by the performing organization, e.g. BRL-1234; AFWL-TR-85-4017-Vol-21-PT-2.

9. SPONSORING/MONITORING AGENCY NAME(S) AND ADDRESS(ES). Enter the name and address of the organization(s) financially responsible for and monitoring the work.

10. SPONSOR/MONITOR'S ACRONYM(S). Enter, if available, e.g. BRL, ARDEC, NADC.

11. SPONSOR/MONITOR'S REPORT NUMBER(S). Enter report number as assigned by the sponsoring/ monitoring agency, if available, e.g. BRL-TR-829; -215.

12. DISTRIBUTION/AVAILABILITY STATEMENT. Use agency-mandated availability statements to indicate the public availability or distribution limitations of the report. If additional limitations/ restrictions or special markings are indicated, follow agency authorization procedures, e.g. RD/FRD, PROPIN, ITAR, etc. Include copyright information.

13. SUPPLEMENTARY NOTES. Enter information not included elsewhere such as: prepared in cooperation with; translation of; report supersedes; old edition number, etc.

14. ABSTRACT. A brief (approximately 200 words) factual summary of the most significant information.

15. SUBJECT TERMS. Key words or phrases identifying major concepts in the report.

16. SECURITY CLASSIFICATION. Enter security classification in accordance with security classification regulations, e.g. U, C, S, etc. If this form contains classified information, stamp classification level on the top and bottom of this page.

17. LIMITATION OF ABSTRACT. This block must be completed to assign a distribution limitation to the abstract. Enter UU (Unclassified Unlimited) or SAR (Same as Report). An entry in this block is necessary if the abstract is to be limited.

The Final Report for the ASU/ARL AFOSR Program

Multicolor (UV-IR) photodetectors based on lattice-matched 6.1 Å II/VI and III/V semiconductors

Award No.: FA9550-10-1-0129

Period 4/1/2012-5/14/2015

PI: Yong-Hang Zhang
Director, Center for Photonics Innovation
&
Fulton Entrepreneurial Professor, School of Electrical, Computer and Energy Engineering
Arizona State University
Tempe, AZ 85287
Tel: 480-965-2562
Fax: 480-965-0775
E-Mail: yhzhang@asu.edu

Project Objectives

- This program focused on the study and demonstration of a novel idea to use optical biasing for multi-color detection using two-terminal monolithically integrated multi-junction photodetectors (MJPDs) [1].
- Multicolor photodetectors and focal plane arrays (FPAs) covering a very broad spectral range from UV to far infrared are highly desirable for not only defense applications but also commercial needs [1]. However, even after several decades of persistent efforts by the global optoelectronics community, such UV-IR photodetection systems still use many different materials that are grown on a diverse array of substrates in order to obtain the high material quality necessary for device applications.
- As a result of the diversity of materials being used, it has been extremely challenging to integrate all of them monolithically without sacrificing device performance [1]. It has been a dream of the photonics community to achieve integration of all devices and systems on a single substrate.
- These integrated semiconductor binaries and their alloys have direct band gaps covering the entire energy spectrum from far IR (~0 eV) to UV (~3.4eV) [1]. Such a unique material platform offers unlimited degrees of freedom for integrating almost any kind of photonic devices (such as lasers, photodetectors, and solar cells) and electronic devices onto a single substrate without large numbers of misfit dislocations to ensure the best material quality. This feature is not achievable by any other known lattice-matched semiconductors on any available substrates.
- We envision that a new generation of multicolor photodetectors and FPAs can be monolithically integrated on a *single chip* with superior device characteristics [1]. Such integrated photonic devices and systems will not only deliver the long-promised potential of revolutionary new levels of performance but will also have additional unprecedented functionalities, far beyond the capabilities of conventional photodetectors and FPAs.
- Figure 1 shows a schematic example of a two terminal (3 detector) multicolor detector under optical bias, which allows the optical addressing to function.

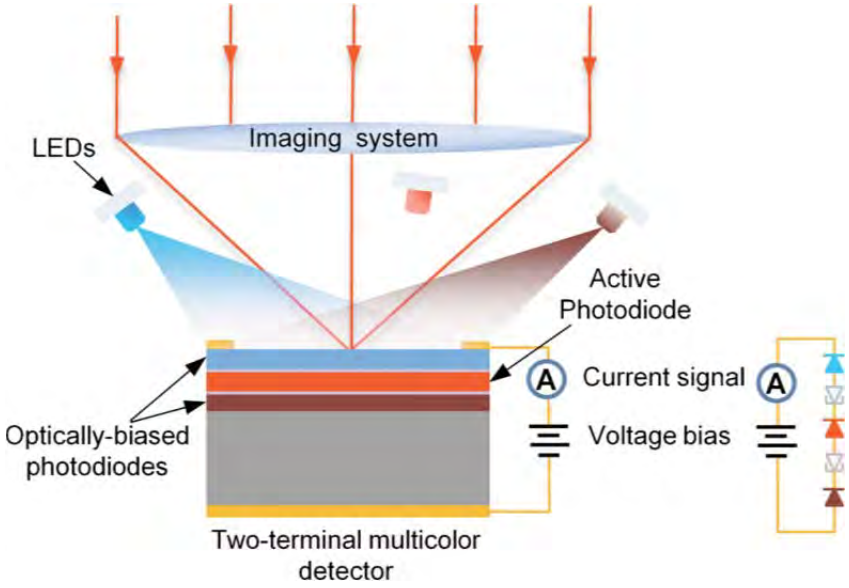

Figure 1 Schematic of the optically addressed, two-terminal, multicolor photodetector. The detector structure consists of multiple photodiodes with different cutoff wavelengths connected in series with tunnel diodes between adjacent photodiodes. The LEDs optically bias the inactive photodiodes in the detector to enable single color detection. Figure from Ref. [2].

Results

- This section outlines some of the key results obtained during this project, including initial demonstrations of optical addressing, tunnel junction studies and multicolor device characterization.

Initial Results and Optical Addressing

- To initially demonstrate this device concept, a commercial InGaP/InGaAs/Ge triple-junction solar cell 22 cm^2 was used as the multicolor photodetector because the solar cell structure is almost identical to the proposed multicolor photodetector design [2].
- The "dark" current densities versus voltage (*J-V*) curves are shown in Figure 2 [2]. The forward and reverse bias regions of the individual active photodiodes' *J-V*s are clearly discernable. The magnitude of the dark current increases as the photodiode's band gap decreases, as expected. The operating point of the active photodiode on the reverse bias portion of its *J-V* curve depends on the voltage and light bias conditions, which can be selected to minimize the dark current.

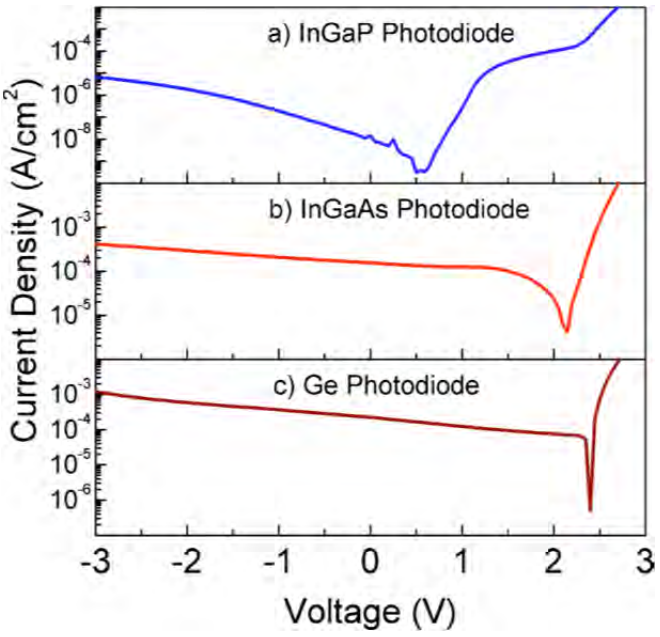

Figure 2 Dark current densities vs. voltage. The *J-V*s were measured with matching optical bias photon flux on the inactive photodiodes and no input signal to the active photodiode. The voltage is across the entire device, not just the active photodiode. Figure from Ref. [2].

- The responsivity, as shown in Figure 3, of the three photodiodes clearly confirms that optical biasing can address onephotodiode at a time in a multicolor detector with only two terminals [2].When the InGaAs and Ge photodiodes are optically biased, the entire detector response is that of the InGaP photodiode only, with zero response above 650 nm. The In-GaAs photodiode shows a response from 650 to 900 nm, while the Ge photodiode responds at greater than 900 nm.The crosstalk between the InGaP and InGaAs photodiodes and between the InGaAs and Ge photodiodes is a result of (i) luminescence coupling, [3][4](ii) photon flux leakage through the InGaP and InGaAs photodiodes, as they may not be optically thick, and (iii) shunts in one or more of the photodiodes. [5][6]In both cases, the crosstalk responsivity is less than ten percent of the responsivity in the photodiode's intended response range, and this can be further reduced using design modifications.

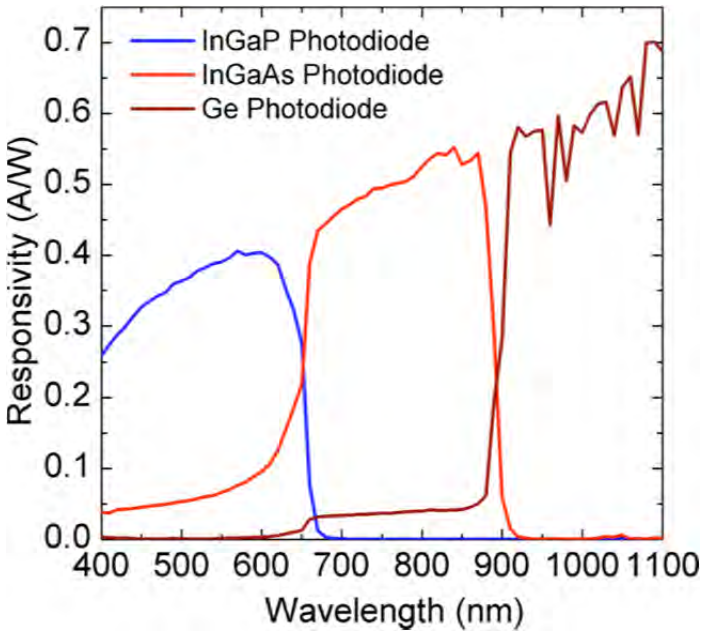

Figure 3 The spectral responsivity curve of each photodiode. The responsivity was measured with matching photon flux on the inactive photodiodes. Figure from Ref. [2].

- The linear dynamic range of the InGaP photodiode covers four orders of magnitude, as shown in Figure 4, under two light bias conditions [2]. The detector current increases linearly as the input signal increases until the photogenerated current due to the signal is larger than the photogenerated current from the light bias. After this point, the detector output saturates due to one of the inactive photodiodes limiting the current. The intensity of the biasing LEDs can limit the upper end of the dynamic range before the detector itself begins to saturate. This is the case in Figure 4, as increasing the light bias by an order of magnitude allows the detector current to continue to increase. The lower detection limit is determined mainly by the noise of the active photodiode.

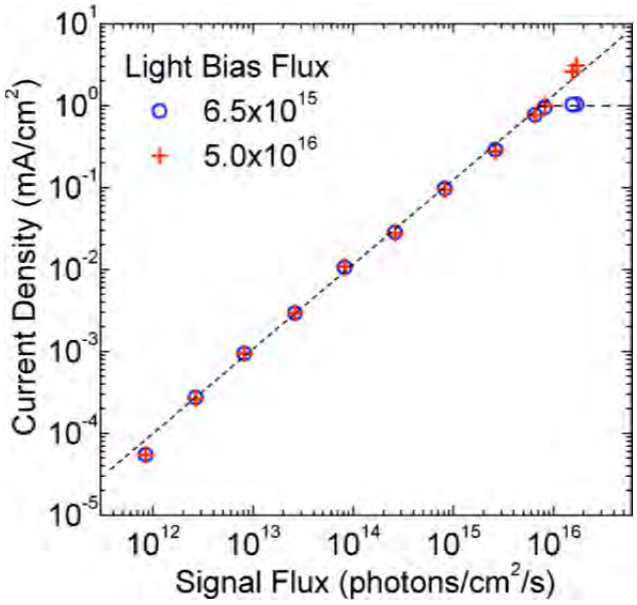

Figure 4 Linear dynamic range of the InGaP photodiode with matching light bias photon flux on the InGaAs and Ge photodiodes. The detector output current saturates after the photogenerated current due to the signal photon flux is larger than the photogenerated current from the light bias photon flux. The dashed lines are guides for the eye. Figure from Ref. [2].

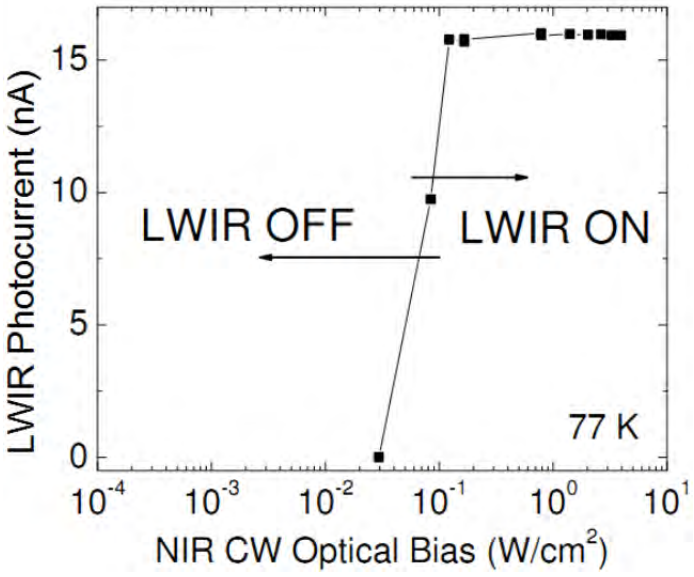

Figure 5 LWIR photocurrent vs. NIR CW optical bias is measured at 77 K. NIR to LWIR band switching threshold of 100 mW/cm2 optical bias is measured at 77 K. Lower band-switching-threshold is observed at lower detector temperatures. Figure from Ref. [7].

- Large-signal NIR peak photocurrent vs. the incident NIR peak power is measured using a 780 nm laser diode with 50%duty cycle at 150 Hz (Figure 5) at 68 K [7]. The NIR photocurrent is measured with a lock-in amplifier and observed to linearly increase over three orders of magnitude until the band-switching threshold of ~3-6 mW/cm2, above which the NIR photocurrent signal saturates and stays constant. Above the threshold, the photodetector enters the LWIR mode of operation and the photocurrent is determined by the LWIR flux.

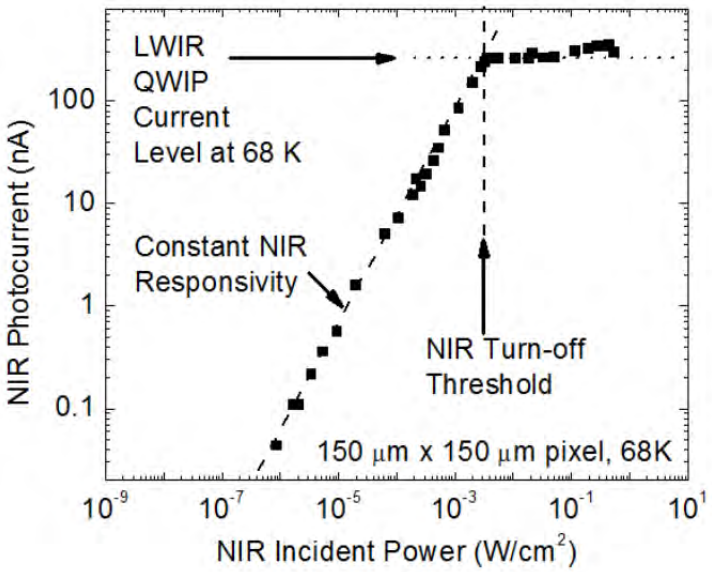

Figure 6 Large-signal NIR peak photocurrent vs. incident peak power at 68 K on a 150 μm x 150 μm sized square pixel. The NIR responsivity is constant until the NIR sub-photodetector turn-off threshold of 3 mW/cm2. Above the threshold, the photodetector enters the LWIR mode of operation and the LWIR QWIP sub-photodetector current limits the photodetector current. Figure from Ref. [7].

- Large-signal characteristics are measured with a single 780 nm laser diode at 100% modulation factor and 50% duty cycle [7]. Small-signal characteristics are also measured with small NIR modulated light from a 780 nm LED, on top of the CW optical bias from a 780 nm laser diode. Both the large-signal and small-signal characteristics are consistent, which shows the linearity in the NIR mode of operation on a wide range of NIR flux.

III-V/II-VI heterostructure tunnel junction and multicolor photodetector results

- Heterovalent interfaces, such as ZnSe/GaAs, ZnTe/GaSb, and CdTe/InSb, contain rich physics in their growth and optical/transport properties. Interest in III-V/II-VI material systems includes both the desire to use III-V substrates for II-VI material epitaxial growth, and the possibility of developing novel optoelectronic devices utilizing III-V/II-VI heterojunctions such as multi-color photodetectors and solar cells [2]. Mixing lattice-matched II-VI and III-V semiconductors could be an efficient way to tune the material properties (e.g. band gap) for specific applications. High-quality monocrystalline CdTe/MgCdTe double heterostructures grown on (001) InSb substrates by molecular beam epitaxy (MBE) have recently been demonstrated with record-long minority

carrier lifetimes of up to 2.7 μs for various structures [8-9]; close to the best values reported for GaAs-based heterostructures. However, limited work on the vertical transport across the CdTe/InSb heterovalent interface has been reported. The investigation of interface properties and vertical transport across the CdTe/InSb heterovalent interface, which has a small lattice mismatch of only 0.03%, is important for future III-V/II-VI quantum well and superlattice structure applications.

- Two samples, an n-CdTe/n-InSb and an n-CdTe/p-InSb heterostructure, both on n-InSb substrates, were grown for transport study using a dual-chamber MBE system equipped with a III-V and a II-VI growth chamber connected by a UHV transfer chamber. The substrate is doped with Te at a concentration of 2×10^{17} cm^{-3} while the n-CdTe, n-InSb and p-InSb epilayers are doped at concentrations of $1\times10^{17}cm^{-3}$, 5×10^{18} cm^{-3} and 1×10^{19} cm^{-3} with In, Te and Be, respectively. In was used as the CdTe ohmic metal contact while Ti/Au was deposited on the InSb. The results of the current-voltage (I-V) measurements with different device areas show ohmic behavior with a small resistivity of <0.1 $\Omega\cdot cm^2$. More comprehensive heterovalent interface characterization is under-going, including electrochemical capacitance voltage, X-ray diffraction, transmission electron microscopy, and Raman scattering.

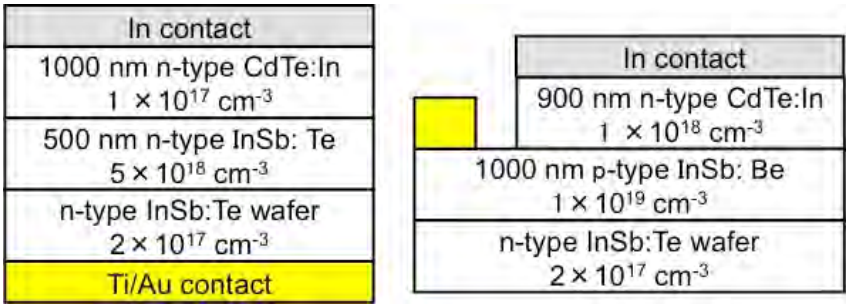

Figure 7 Schematic layer structures of n-CdTe/n-InSb and n-CdTe/p-InSb vertical transport samples. The device areas range from 0.4×0.4 mm^2 to 5×5 mm^2.

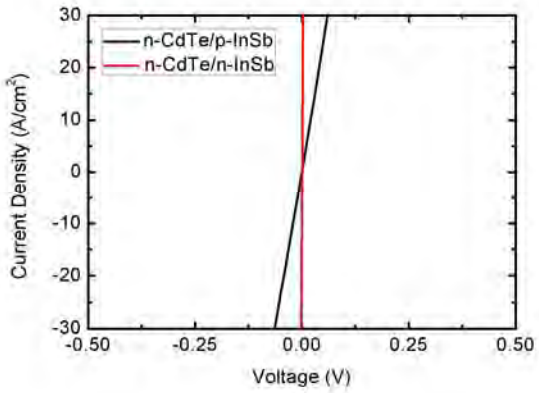

Figure 8 Current-voltage characteristics of n-CdTe/n-InSb and n-CdTe/p-InSb vertical transport samples show linear behaviors with small resistivity below 0.1 $\Omega\cdot cm^2$ indicating negligible voltage drop across interfaces.

- With the InSb/CdTe tunnel junction demonstrated, we moved one step forward to make an InSb/CdTe optically-addressed visible-and-infrared two-color photodetector (see figure 9). It is

comprised of a CdTe nBn sub-photodetector (820 nm band gap), and an InSb PIN sub-photodetector (7 μm band gap) that is well studied as Reference 10. The nBn detector is a novel photodetector structure [11] designed to suppress the dark current without damping the photocurrent in the realm of infrared photo detection. The first letter n denotes an n-type contact layer, the second letter n denotes an n-type absorber layer, and B denotes a barrier layer, which is normally composed of a wide-band-gap material with large conduction-band offset to the absorber layer to block the majority electrons but negligible valence-band offset to allow the minority (photogenerated) holes from the absorber layer to pass freely. The nBn detector structure has never been explored for visible light detection materials to the author's knowledge, even though it has been broadly applied for a variety of infrared detection materials such as InAsSb [12], HgCdTe [13], InAs/GaSb superlattice [14], and InAs/InAsSb superlattice [15]. Here, we use a 20 nm thick ZnTe as the barrier layer to demonstrate a CdTe nBn photodetector. ZnTe has a considerable conduction band offset of ~ 1 eV to serve as an electron barrier, and a small valence band offset of ~ 0.1 eV to almost perfectly align the valance band edge to the CdTe absorber[16]. The 20 nm ZnTe is thick enough to suppress electron direct-tunneling current according to our calculation, and also, it is thin enough to minimize the lattice-mismatch induced dislocations that could propagate into the CdTe absorber and degrade its optical and electrical properties. The 1 μm CdTe absorber can absorb 99 % of the incident photons with energy greater than its bandgap and thus the amount of residue visible light that could be absorbed by the InSb detector is minimized. Indium is deposited on the mesa top and annealed at 200 ° C for 1 min to make an Ohmic contact to CdTe, and Ti/Pt/Au was deposited on the back of the n-type InSb substrate to make an ohmic contact to InSb.

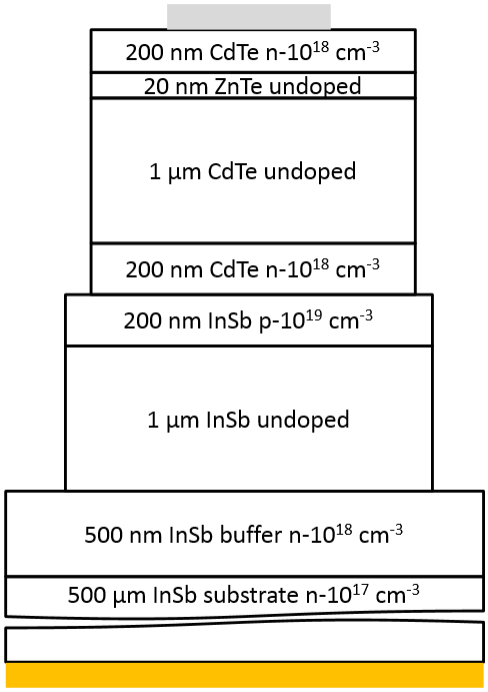

Figure 9 The layer structure of the CdTe/InSb optically-addressed visible-and-infrared two-color photodetector.

- Stand-alone CdTe nBn photodetector and InSb PIN photodetector were grown, fabricated and characterized for reference purpose. Figure 10 shows, the resistance of the (n+)-CdTe/(p+)-InSb hetero-structure is indeed much lower than either the CdTe nBn photodetector or the InSb PIN photodetector at both room temperature and 78 K, suggesting that the voltage loss at the CdTe/InSb interface is negligible in the integrated multi-color photodetector. Even though the InSb PIN photodetector suffers from surface leakage current at 77 K, further silicon oxide surface passivation can be done to suppress the surface leakage [10] in the future work.

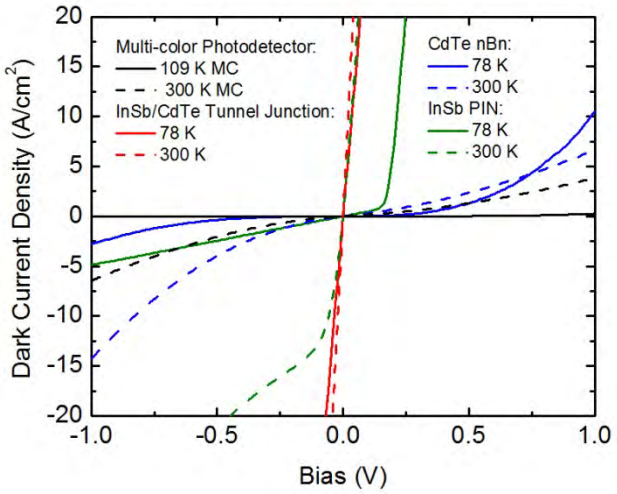

Figure 10 The dark I-V curves for the CdTe/InSb multicolor photodetector, the stand-alone CdTe nBn photodetector, the stand-alone InSb PIN photodetector and the InSb/CdTe tunnel junction at room temperature and liquid nitrogen cooling temperatures.

- The multi-color photodetector is at CdTe detection mode in default at room temperature without any optical addressing bias. This is as the expected because the resistance of the CdTe nBn sub-photodetector is much greater than that of the InSb PIN sub-photodetector, and the InSb PIN infrared sub-photodetector itself has very low responsivity at room temperature. The optical addressing is difficult at room temperature: one cannot turn on the InSb sub-detector using an 808 nm CW laser with a power up to 2 W/cm^2. On the other hand, at 77 K which is the practical working temperature for the InSb sub-photodetector, the multi-color detector has shown optical addressing behavior. One can enhance its infrared response by 30 times under a 3.39 μm light source using a 633 nm CW laser as the optical bias with a power of 0.08 W/cm^2.

Detailed characterization for the CdTe/ZnTe/CdTe nBn photodetector

- The novel CdTe/ZnTe/CdTe nBn photodetector has shown high gain, non-linearity, and slow response at room temperature. Rigorous measurements show that the external quantum efficiency (EQE) of the CdTe/ZnTe/CdTe nBn photodetector can be much higher than 100% as under a relatively low light power of 10^{-8} – 10^{-6} W, seen in Figure 11, indicating a gain effect is present in the device. The EQE was determined by measuring the photocurrent under a 633 nm laser light confined onto the pixel under test only using an optical fiber. The light power was calibrated using a silicon detector with a calibrated EQE spectrum.

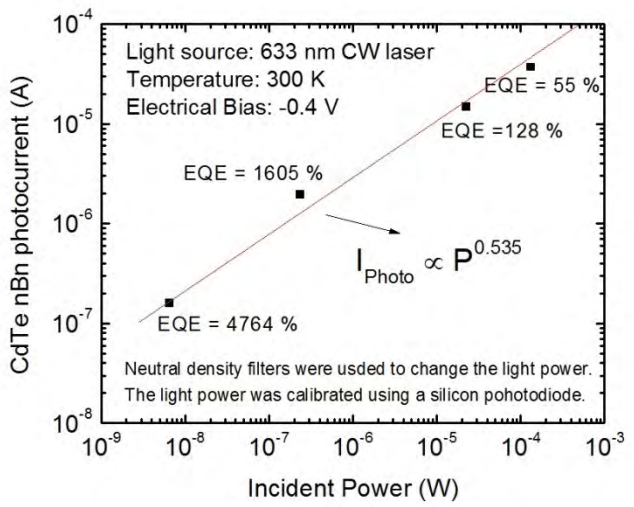

Figure 11 The CdTe/ZnTe/CdTe nBn photodetector has an external quantum efficiency (EQE) much higher than 100 %, with a non-linear photocurrent vs. light power relation which can be fitted using a power law of $I_{Photo} = AP^{0.535}$.

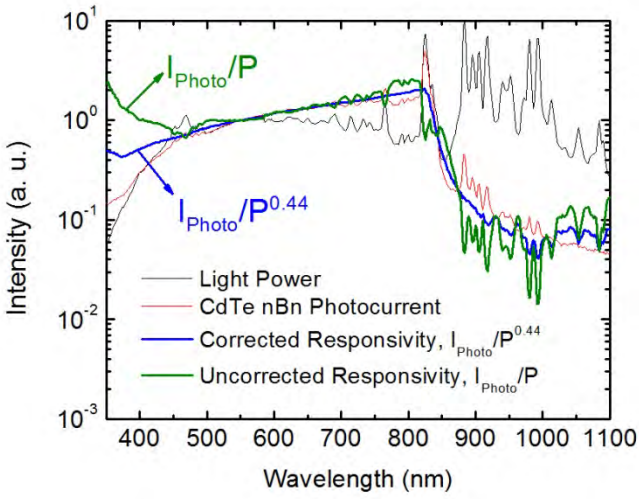

Figure 12 Uncalibrated Responsivity spectra of the CdTe/ZnTe/CdTe nBn photodetector. The nonlinear relation between the input light power and photocurrent must be handled to get a smooth responsivity curve.

- The photodetector is nonlinear with a photocurrent vs. light power relation following a power law as Figure 11. This nonlinearity must be considered for the responsivity spectrum measurement. As Figure 12, the conventional definition I_{photo}/P of the responsivity appears to be very spiky as a function of wavelength. This is due to the nonlinearity of the photodetector and the peaks in the power spectrum of the light source. In comparison, an $I_{photo}/P^{0.44}$ spectrum appears to be much smoother. The nonlinearity of the CdTe nBn photodetector can be summarized using the following formula.

$$I_{photo} = A(\lambda)P^{0.5} \quad (1)$$

where A is a constant that is dependent of the wavelength λ only, P is the light power, and I_{photo} is photocurrent. This power law suggests the presence of Urbach tail at the band edges according to Rose [17], if the Urbach tail states have an exponential distribution in energy such that

$$N_t(E_t) = Aexp\left(-\frac{|E_t - E_c|}{kT_1}\right) \quad (2)$$

Where A is a constant, E_C is the conduction band edge, and the temperature, T_1, is a formal parameter that can be adjusted to make the density of states vary more or less rapidly with energy [17]. As the incident light power increases, more and more Urbach tail states fall between the electron and hole quasi Fermi levels and become recombination centers. As a consequence, the carrier recombination process is enhanced as the light power increases and less portion of the photogenerated carriers are extracted. It can be derived that [17]

$$I_{photo} \propto P^{T_1/(T+T_1)} \quad (3)$$

- The photocurrent of the CdTe nBn photodetector has an exponential decay tail of ~ 3 ms after the light source is electrically turned off, suggesting the existence of slow carrier trapping processes that can induce photoconductive gain.

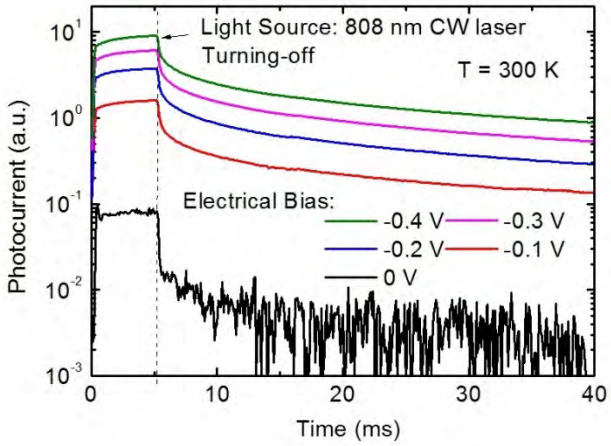

Figure 13 The long photocurrent decay tail of ~ 3 ms indicates the existence of slow carrier trapping processes which can induce significant photoconductive gain.

- The photoluminescence measurement of CdTe/MgCdTe double-heterostructures with different CdTe doping concentrations can shed some light on the device physics. As Figure 14, it is shown that undoped CdTe has very little sub-band-gap optical transition; however, heavily doped n-type CdTe have significant sub-band-gap optical transition due to the induced Urbach tail states. In our CdTe nBn photodetector, the absorber layer is undoped and the top contact layer is heavily doped as n-type with a concentration of 10^{18} cm^{-3}. It is then suggested that the ZnTe barrier layer may not block the photogenerated electrons from the top contact layer very well, because under a

negative bias on the top, the photodetector has the sub-band-gap photo response signature (Figure 14) coming from the top contact layer. This was impossible if the ZnTe layer fully blocked the electrons according to our numerical simulation. Our simulation has shown that, if the barrier layer can fully block the electrons, with a negative bias applied on the top, the photo response comes from the absorber exclusively. Meanwhile, if a positive bias is applied on the top, the photo response exclusively originates from the top contact layer. Such phenomenon was experimentally observed in a bias-addressed two-color pBp infrared photodtector [18].

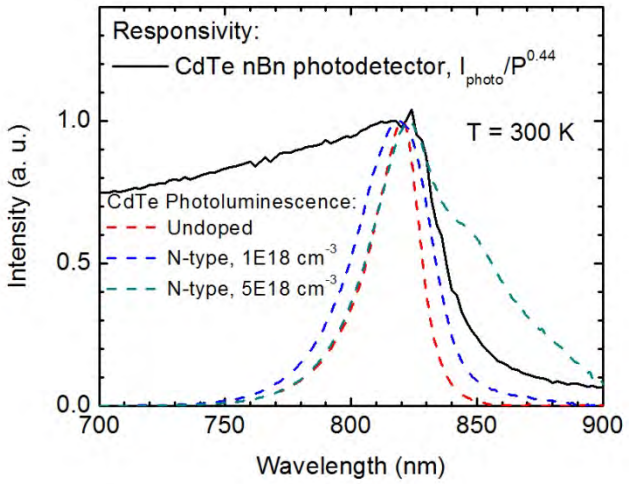

Figure 14 The photoluminescence measurement shows that the sub-band-gap photo response of the CdTe nBn photodetector is the signature of the top contact layer with heavy n-type doping, suggesting that the ZnTe barrier layer cannot fully block the electrons.

- The device physics of the CdTe nBn photodetector can be now preliminarily understood. Firstly, the high dark current of 1 A/cm^2 under the bias of -0.4 V at room temperature can be attributed to electron current because the ZnTe layer cannot fully block the electrons as the designed. Secondly, with a poor electron-blocking barrier layer, the nBn photodetector can have significant photoconductive gain if the holes are trapped and the electrons go through the device for multiple cycles. Lastly, the non-linear relation between the input light power and the photocurrent can be attributed to the Urbach tail states in the heavily doped top contact layer according to Rose's theory [17].

Summary

- Individual color detection is realized with appropriate optical biasing [2]. This concept is demonstrated experimentally using a three-color photodetector and biasing light emitting diodes. The measured linear dynamic range is greater than four orders of magnitude, making it a practical device for a broad range of applications.
- Optical Addressing method shown to work for switching between NIR and LWIR detectors [7].

- (n+)-CdTe/(p+)-InSb and (n+)-CdTe/(n+)-InSb hetero-structure measured to be effective tunneling junctions, making it possible to achieve a multi-color photodetector compised of a CdTe sub-photodetector and an InSb sub-photodetector.
- A CdTe/InSb multi-color photodetector has been designed, grown, fabricated and characterized. Optical addressing have preliminarily realized at the temperature of 77 K. The infrared photo responsivity can be enhanced by 30 times using an optical bias of 633 nm CW laser with the power of 0.08 W/cm^2.
- A gain greater than unity, a non-linear photocurrent vs. photon power behavior and a slow photo response have been observed and confirmed in the CdTe/ZnTe/CdTe nBn photodetector.
- The device physics has been preliminarily clarified for the CdTe/ZnTe/CdTe nBn photodetector.

References

[1] Y-H. Zhang, "Optically biased monolithically integrated multicolor photodetectors", AFOSR proposal.

[2] E. H. Steenbergen, M. J. DiNezza, W. H. G. Dettlaff, S. H. Lim, and Y.-H. Zhang, "Optically-addressed two terminal multicolor photodetector", Appl. Phys. Lett. 97(16), 161111 (2010).

[3] C. Baur, M. Hermle, F. Dimroth, and A. W. Bett, "Effects of optical coupling in III-V multilayer systems", Appl. Phys. Lett. 90,192109 (2007).

[4] H. Yoon, R. R. King, G. S. Kinsey, S. Kurtz, and D. D. Krut, *Proceedings of the 3rd World Conference on Photovoltaic Energy Conversion* (Arisumi Printing, Inc., Japan, 2003), p. 745.

[5] M. Meusel, C. Baur, G. Letay, A. W. Bett, W. Warta, and E. Fernandez, "Spectral response measurements of monolithic GaInP/Ga(In)As/Ge triple-junction solar cells: Measurement artifacts and their explanation", Prog. Photovoltaics 11, 499 (2003).

[6] S. H. Lim, K. O'Brien, E. H. Steenbergen, J.-J. Li, and Y.-H. Zhang, Proceedings of the 35th IEEE PVSC (unpublished).

[7] O.O. Cellek, H.S. Kim, J.L. Reno and Y.-H. Zhang. "NIR/LWIR Dual-band Infrared Photodetectors with Optical Addressing", Proc. of SPIE Vol. 8353 83533E-1-6, (2012).

[8] M. J. DiNezza, X.-H. Zhao, S. Liu, A. P. Kirk, and Y.-H. Zhang, "Growth, steady-state and time-resolved photoluminescence study of CdTe/MgCdTe double heterostructures on InSb substrates using molecular beam epitaxy", Appl. Phys. Lett. 103, 193901 (2013).

[9] X.-H. Zhao, M. J. DiNezza, S. Liu, S. Lin, Y. Zhao, and Y.-H. Zhang, "Time-resolved and excitation-dependent photoluminescence study of CdTe/MgCdTe double heterostructures grown by molecular beam epitaxy", JVST B 32, 040601 (2014).

[10] J. Abautret, A. Evirgen, J.P. Perez, P. Christol, A. Rouvié, R. Cluze, A. Cordat, J. Rothman, "Design, fabrication, and characterization of InSb Avalanche Photodiode", Proc. of SPIE Vol. 8993 899314-1, (2014).

[11] S. Maimon and G. W. Wicks, "nBn detector, an infrared detector with reduced dark current and higher operating temperature", Appl. Phys. Lett. 89, 151109 (2006).

[12] A. Soibel, C. J. Hill, S. A. Keo, L. Hoglund, R. Rosenberg, R. Kowalczyk, A. Khoshakhlagh, A. Fisher, D. Z.-Y. Ting, and S. D. Gunapala, "Room temperature performance of mid-wavelength infrared InAsSb nBn detectors", Appl. Phys. Lett. 105, 023512 (2014).

[13] A. M. Itsuno, J. D. Phillips, and S. Velicu, “Mid-wave infrared HgCdTe nBn photodetector”, Appl. Phys. Lett. 100, 161102 (2012).
[14] J. B. Rodriguez, E. Plis, G. Bishop, Y. D. Sharma, H. Kim, L. R. Dawson, and S. Krishna, “nBn structure based on InAs/GaSb type-II strained layer superlattices”, Appl. Phys. Lett. 91, 043514 (2007).
[15] H. S. Kim, O. O. Cellek, Z.-Y. Lin, Z.-Y. He, X.-H. Zhao, S. Liu, H. Li, and Y.-H. Zhang, “Long-wave infrared nBn photodetectors based on InAs/InAsSb type-II superlattices”, Appl. Phys. Lett. 101, 161114 (2012).
[16] Chris G. Van de Walle and J. Neugebauer, “Universal alignment of hydrogen levels in semiconductors, insulators and solutions”, Nature, VOL 423, (2003).
[17] A. Rose, “Concepts in Photoconductivity and Allied Problems”, 2nd Edition, Krieger Publishing Company, New York, (1978).
[18] Y.-F. Lao, P. K. D. D. P. Pitigala, A. G. Unil Perera, E. Plis, S. S. Krishna, and P. S. Wijewarnasuriya, “Band offsets and carrier dynamics of type-II InAs/GaSb superlattice photodetectors studied by internal photoemission spectroscopy”, Applied Physics Letters 103, 181110 (2013).

Publication List

Journal Publications

1. X.-M. Shen, H. Li, S. Liu, D. J. Smith, Y.-H. Zhang, Study of InAs/InAsSb type-II superlattices using high-resolution x-ray diffraction and cross-sectional electron microscopy, J. of Cryst. Growth 381, 1-5 (2013).
2. J. Fan, X. Liu, L. Ouyang, R. E. Pimpinella, M. Dobrowolska, J. K. Furdyna, D. J. Smith, and Y.-H. Zhang, “Molecular beam epitaxial growth of high-reflectivity and broad-bandwidth ZnTe/GaSb distributed Bragg reflectors”, J. Vac. Sci. Technol. B 31, 03C109 (2013).
3. J. Fan, L. Ouyang, X. Liu, J. K. Furdyna, D. J. Smith, and Y.-H. Zhang, “GaSb/ZnTe double-heterostructures grown using molecular beam epitaxy”, J. of Crystal Growth 371 (1), 122–125 (2013).
4. S. Liu, H. Li, O. O. Cellek, D. Ding, X.-M. Shen, E. H. Steenbergen, Z.-Y. Lin, J. Fan, Z.-Y. He, J. Lu, S. R. Johnson, D. J. Smith, and Y.-H. Zhang, “Impact of substrate temperature on the structural and optical properties of strain-balanced InAs/InAsSb type-II superlattices grown by molecular beam epitaxy”, Appl. Phys. Lett. 102, 071903-071903-4 (2013).
5. H. Li, S. Liu, O. O. Cellek, D. Ding, X.-M. Shen, E. H. Steenbergen, J. Fan, Z. Lin, Z.-Y. He, Q. Zhang, P. T. Webster, S. R. Johnson, L. Ouyang, D.J. Smith, and Y.-H. Zhang, “A calibration method for group V fluxes and impact of V/III flux ratio on the growth of InAs/InAsSb type-II superlattices by molecular beam epitaxy”, J. of Crystal Growth 378, 145-149 (2013).
6. H.S. Kim, O.O. Cellek, Z. Lin, Z.-Y. He, H. Li, S. Liu, and Y.-H. Zhang, “Long-wave infrared nBn photodetectors based on InAs/InAsSb type-II superlattices”, Applied Physics Letters 101, 161114 (2012).
7. O.O. Cellek, J.L. Reno, Y.-H. Zhang, “Optically addressed near and long-wave infrared multiband photodetectors”, Applied Physics Letters 100, 241103-241103. (2012)

8. X. Liu, D. J. Smith, H. Cao, Y. P. Chen, J. Fan, Y.-H. Zhang, R. E. Pimpinella, M. Dobrowolska, and J. K. Furdyna, “Characterizations of Bi2Te3 and Bi2Se3 topological insulators grown by MBE on (100) GaAs substrates”, J. Vac. Sci. Technol. B 30, 02B103 (2012);

9. M. J. DiNezza, Q. Zhang, D. Ding, J. Fan, X. Liu, J. K. Furdyna, Y.-H. Zhang, “Aluminum diffusion in ZnTe films grown on GaSb substrates for n-type doping”, physica status solidi (c), 9, 1720–1723 (2012).
10. Q. Zhang, X. Liu, M. J. DiNezza, J. Fan, D. Ding, J. K. Furdyna, Y.-H. Zhang, “Influence of Te/Zn flux ratio on Aluminum doped ZnTe grown by MBE on GaSb substrates”, physica status solidi (c), 9, 1724–1727 (2012).
11. E. H. Steenbergen, K. Nunna, L. Ouyang, B. Ullrich, D. L. Huffaker, Y.-H. Zhang, “Strain-balanced InAs/InAs1-xSbx type-II superlattices grown by molecular beam epitaxy on GaSb substrates”, J. Vac. Sci. Technol. B 30, 02B107 (2012);
12. J. Fan, L. Ouyang, X. Liu, D. Ding, J. K. Furdyna, D. J. Smith, and Y.-H. Zhang, “Influence of temperature ramp on the materials properties of GaSb grown on ZnTe using molecular beam epitaxy”, J. Vac. Sci. Technol. B, 30, 02B122 (2012).
13. E. H. Steenbergen, B. C. Connelly, G. D. Metcalfe, H. Shen, M. Wraback, D. Lubyshev, Y. Qiu, J. M. Fastenau, A. W. K. Liu, S. Elhamri, O. O. Cellek, and Y.-H. Zhang, “Significantly improved minority carrier lifetime observed in a long-wavelength infrared III-V type-II superlattice comprised of InAs/InAsSb”, Appl. Phys. Lett. 99, 251110 (2011).
14. X. Liu, D. J. Smith, J. Fan, Y.-H. Zhang, H. Cao, Y. P. Chen, J. Leiner, B. J. Kirby, M. Dobrowolska, and J. K. Furdyna, “Structural properties of Bi2Te3 and Bi2Se3 topological insulators grown by molecular beam epitaxy on GaAs(100) substrates”, Appl. Phys. Lett. 99, 171903 (2011).
15. E. H. Steenbergen, Y. Huang, J.-H. Ryou, L. Ouyang, J.-J. Li, D. J. Smith, R. D. Dupuis, Y.-H. Zhang, “Structural and optical characterization of type-II InAs/InAs1-xSbx superlattices grown by metalorganic chemical vapor deposition”, Appl. Phys. Lett. 99, 071111 – 071114 (2011).

16. E. H. Steenbergen, M. J. DiNezza, W. H. G. Dettlaff, S. H. Lim, Y.-H. Zhang, “Effects of varying light bias on an optically-addressed two-terminal multi-color photodetector”, Infrared Physics and Technology 54, 292-295 (2011).
17. Y. Huang, J.-H. Ryou, R. D. Dupuis, V. R. D’Costa, E. H. Steenbergen, J. Fan, Y.-H. Zhang, A. Petschke, M. Mandl, S.-L. Chuang, “Epitaxial growth and characterization of InAs/GaSb and InAs/InAsSb type-II superlattices on GaSb substrates by metalorganic chemical vapor deposition for long wavelength infrared photodetectors”, J. of Cryst. Growth 314, 92-96 (2011).
18. J. Fan, L. Ouyang, X. Liu, D. Ding, J.K. Furdyna, D. J. Smith and Y.-H. Zhang, “Growth and material properties of ZnTe on GaAs, InP, InAs and GaSb (0 0 1) substrates for electronic and optoelectronic device applications”, J. of Cryst. Growth 323, 127-131 (2010).
19. E. H. Steenbergen, M. J. DiNezza, W. H. G. Dettlaff, S. H. Lim, Y.-H. Zhang, “Optically-addressed two-terminal multi-color photodetector”, Appl. Phys. Lett. 97 161111-161114 (2010).

Conference Presentations

1. P. T. Webster, J. Lu, N. A. Riordan, E. H. Steenbergen, S. Liu, D. J. Smith, Y.-H. Zhang, and S. R. Johnson, “Optical Properties of InAs/InAsSb Superlattices Grown With and Without Bi as a Surfactant”, presented at 18th International MBE Conference, Flagstaff, AZ, September 8-12, 2014.
2. Z.-Y. Lin, X.-M. Shen, S. Liu, H. Li, J. D. Justice, T. Detchprohm, R. D. Dupuis, D. J. Smith, and Y.-H. Zhang, “Comparison on Structural and Optical Properties of Strain-Balanced InAs/InAsSb Type-II Superlattices Grown by MBE and MOCVD on GaSb Substrates”, presented at 18th International MBE Conference, Flagstaff, AZ, September 8-12, 2014.
3. J. Lu, M.J. DiNezza, X.-H. Zhaoi, S. Liu, Y.-H. Zhang, and D.J. Smith, “TEM study of defects and interfaces of epitaxial CdTe and InSb layers grown on InSb(001) substrates, presented at International MBE Conference”, presented at International MBE Conference, Flagstaff, September 8-12, 2014.
4. J. Lu, P.T. Webster, S. Liu, S.R. Johnson, Y.-H. Zhang, and D.J. Smith, “Investigation of Bi incorporation and droplet formation in MBE-grown InAsBi by transmission electron microscopy”, presented at International MBE Conference, Flagstaff, September 8-12, 2014.
5. J. Lu, X.-M. Shen, Y.-H. Zhang, and D.J. Smith,“Quantitative study of compositional uniformity abd interfacial starin in InAs/InAsxInAsSb1-x Type-II superlattices”, presented at Microscopy and Microanalysis 2014, Hartford, CT, August 2-6, 2014.
6. Zhao-Yu He, Oray O. Cellek, Shi Liu, Xiao-Meng Shen, Zhi-Yuan Lin, and Yong-Hang Zhang, “Mid-wave infrared nBn photodetectors using InAs/InAsSb type-II superlattices” Quantum Strcutured Infrared Photodetector International Conference, Santa Fe, NM, July 2014
7. Jing Lu, Elizabeth H. Steenbergen, Xiao-Meng Shen, Shi Liu, Yong-Hang Zhang, David J. Smith, “Compositional Uniformity and Interfacial Gradient in InAs/InAs1-xSbx Type-II Superlattices by Electron Microscopy”, 30th North American Molecular Beam Epitaxy Conference, Banff, Canada, Oct. 5-11, 2013.
8. Z.-Y. He, O. O. Cellek, S. Liu, H. S. Kim, J. Fan, Z.-Y. Lin, and Y.-H. Zhang, “Designs and Characteristics of Infrared nBn Photodectors based on InAs/InAsSb Type-II Superlattices”, SPIE Defense, Security, and Sensing, Baltimore, 29 April - 3 May, 2013.
9. J. Fan, Z.-Y. Lin, O. O. Cellek, S. Liu, and Y.-H. Zhang, “Study of Shockley-Read-Hall, radiative, and Auger recombination processes in InAs/InAsSb type-II superlattices”, SPIE Defense, Security, and Sensing, Baltimore, 29 April - 3 May, 2013.
10. J.-J. Li and Y.-H. Zhang, “Accurate measurement of external quantum efficiency of multi-junction solar cells, Space Power Workshop”, Manhattan Beach, CA, April 2013
11. O. O. Cellek, Z.-Y. He, Z.-Y. Lin, H. S. Kim, S. Liu, and Y.-H. Zhang, “InAs/InAsSb type-II superlattice infrared nBn photodetectors and their potential for operation at high temperatures”, SPIE Photonics West, San Francisco, Feb. 2-8, 2013.
12. X.-M. Shen, H. Li, S. Liu, D. J. Smith, and Y.-H. Zhang, “Structural characterization of InAs/InAs1-xSbx type-II superlattices grown by molecular beam epitaxy”, The 29th NAMBE Conference, 14-17 October, 2012. (Best poster award)
13. P. T. Webster, A. R. Sharma, H. Liang, N. A. Riordan, O. O. Cellek, E. H. Steenbergen, X.-M. Shen, H. Li, S. Liu, D. Ding, Q. Zhang, Y.-H. Zhang, and S. R. Johnson, “Investigation of the Mid and Long IR Optical Properties of Type-II InAs/InAsSb Superlattices using Spectroscopic Ellipsometry”, The 29th NAMBE Conference, 14-17 October, 2012.

14. H. Li, D. Ding, O.O. Cellek, S. Liu, X.-M. Shen, E. H. Steenbergen, J. Fan, Z.-Y. Lin, Z.-Y. He, Q. Zhang, M. J. DiNezza, W. Hank G. Dettlaff, J.-J. Li, P. T. Webster, S. R. Johnson, D. J. Smith, and Y.-H. Zhang, "Molecular beam epitaxy growth of InAs/InAsSb type-II superlattices for infrared applications", The 17th International Conference on Molecular Beam Epitaxy, 23-28 September, 2012.
15. P. T. Webster, N. A. Riordan, H. Liang, O. O. Cellek, E. H. Steenbergen, X.-M. Shen, H. Li, S. Liu, D. Ding, Q. Zhang, Y.-H. Zhang, and S. R. Johnson, "Absorption Coefficient of Type-II InAs/InAsSb Superlattices Measured using Spectroscopic Ellipsometry", The 39th International Symposium on Compound Semiconductors, 27-30 August, 2012.
16. H. S. Kim, O. O. Cellek, Z. Lin, Z.-Y. He, X.-H. Zhao, H. Li, S. Liu, and Y.-H. Zhang, "Infrared photodetectors based on MWIR and LWIR InAs/InAsSb superlattices", SPIE Optics + Photonics, 12-16 August 2012.
17. E. H. Steenbergen, B. C. Connelly, G. D. Metcalfe, H. Shen, M. Wraback, D. Lubyshev, Y. Qiu, J. M. Fastenau, A. W. K. Liu, S. Elhamri, O.O. Cellek, and Y.-H. Zhang, "Temperature-dependent minority carrier lifetime of InAs/InAs1-xSbx type-II superlattices", SPIE Optics + Photonics, 12-16 August 2012.
18. E. H. Steenbergen, O. O. Cellek, H. Li, S. Liu, X. Shen, H. S. Kim, Z. Lin, L. Ouyang, D.J. Smith, S.R. Johnson, Yong-Hang Zhang, "InAs/InAsSb superlattices: a promising alternative type-II superlattice material for infrared detection", Quantum Structured Infrared Photodetector International Conference (QSIP 2012), Corsica (France), June 17-22, 2012.
19. O. O. Cellek, E. H. Steenbergen, H. S. Kim, Y.-H. Zhang, and J. L. Reno, "Device Characteristics of Optically-addressed Infrared Photodetectors, Quantum Structured Infrared Photodetector", International Conference (QSIP 2012), Corsica (France), June 17-22, 2012.
20. O. O. Cellek, H. S. Kim, E. H. Steenbergen, H. Li, Z. Lin, S. Liu, Y.-H. Zhang, "MWIR and LWIR photodetectors made of InAs/InAsSb Type-II Superlattices", SPIE Defense, Security, and Sensing, Baltimore, 23 - 27 April 2012.
21. E. H. Steenbergen, O. O. Cellek, H. Li, X. Shen, Z. Lin, D. Ding, S. Liu, Q. Zhang, H. S. Kim, L. Ouyang, J. Fan, Z. He, P. Webster, S. R. Johnson, D. J. Smith, Y.-H. Zhang, "InAs/InAsSb Type-II Superlattice: A Promising Material for Long Wavelength Infrared Applications", SPIE Defense, Security, and Sensing, Baltimore, 23 - 27 April 2012.
22. O. O. Cellek, Y.-H. Zhang, "Optically addressed multiband photodetector for infrared imaging applications", SPIE Photonics West, San Francisco, Jan. 21-26, 2012.
23. E. H. Steenbergen, O. O. Cellek, Y.-H. Zhang, "Valance band offset study for InAs/InAsSb superlattice infrared photodetectors", SPIE Photonics West, San Francisco, Jan. 21-26, 2012.
24. L. Ouyang, E.H. Steenbergen, K. Nunna, D.L. Huffaker, Y.-H. Zhang, and David J. Smith, "Structural properties of InAs/InAs1-xSbx type-II superlattices grown by MBE", 28th North American Molecular Beam Epitaxy conference, San Diego, 2011.
25. E.H. Steenbergen, K. Nunna, B. Ullrich, L. Ouyang, D.J. Smith, D.L. Huffaker and Y.-H. Zhang, "InAs/InxAs1-xSb type-II superlattices for long-wavelength infrared applications", 28th North American Molecular Beam Epitaxy conference, San Diego, Aug. 2011.
26. E.H. Steenbergen, Y. Huang, J.-H. Ryou, R.D. Dupuis, and Y.-H. Zhang, "Optical properties of strain balanced InAs/InxAs1-xSb type-II superlattices", the 15th International Conference on Narrow Gap Systems, Blacksburg, Aug. 2011.

27. O.O. Cellek, E.H. Steenbergen and Y.-H. Zhang, “New concept for optically-addressed two-terminal multi-color detector”, 4th Space Based Sensing and Protection Conference, Kirtland, 2011.
28. E.H. Steenbergen, L. Ouyang, D.J. Smith, Y. Huang, J.-H. Ryou, R.D. Dupuis and Y.-H. Zhang, “Strain-balanced type-II InAs/InAsSb superlattices for infrared photodetectors”, 4th Space Based Sensing and Protection Conference, Kirtland, May 2011.
29. E.H. Steenbergen, V.R. D’Costa, Y. Huang, J. Fan, J.-J. Li, J.-H. Ryou, R.D. Dupuis, Y.-H. Zhang, “InAs/ InAsxSb1-x Type-II Superlattices for LWIR Detectors”, 10th International Conference on Mid-Infrared Optoelectronics: Materials and Devices, Shanghai, September 5-9, 2010
30. Y.-H. Zhang, J. Furdyna, X. Liu, and D. Ding, “MBE growth of 6.1 Å II-VI and III-V semiconductors on GaSb substrates and their potential device applications”, the 16th International Conference on MBE, Berlin, Aug. 22-27, 2010.
31. E. H. Steenbergen, M. J. DiNezza, W. H. G. Dettlaff, S. H. Lim, D. Ding, Y.-H. Zhang, “Optically-biased two-terminal multicolor photodetectors”, Quantum Structure Infrared Photodetector International Conference, Istanbul, Turkey, Aug 15-20, 2010.

Invited talks

1. Y.-H. Zhang, “Ga-Free InAs/InAsSb type-II superlattice: its past, present and future”, SPIE Photonics West, San Francisco, Feb. 2013.
2. Y.-H. Zhang, “Integration of Lattice-Matched 6.1? II-VI/III-V Semiconductors for Optoelectronic Device Applications”, The U.S. Workshop on the Physics and Chemistry of II-VI Materials, Seattle, November 27-29, 2012.
3. Y.-H. Zhang, “IR Detectors Based on Ga-Free InAs/InAsSb type-II Superlattices and Two-Terminal Multi-Color FPAs”, the 7th Annual IDGA’s Night Vision Systems, Arlington, Virginia July 23-25, 2012.
4. O.O. Cellek, H. Li, X.-M. Shen, Z. Lin, E.H. Steenbergen, S. Liu, H.S. Kim, J. Fan, P.T. Webster, L. Ouyang, Z.-Y. He, S.R. Johnson, D.J. Smith, and Y.-H. Zhang, “Ga-free Type-II Superlattices and Optically-Addressed Multi-Color Photodetectors”, The 2012 International Symposium on Optoelectronics Materials & Devices, Chicago, July 12-13, 2012.
5. O. O. Cellek, E. H. Steenbergen, H. Li, H. S. Kim, Z.-Y. Lin, and Y.-H. Zhang, “MWIR and LWIR InAs/InAsSb Type-II Superlattices and optically-addressed multicolor photodetectors”, SPIE Defense, Security, and Sensing, Baltimore, April 2012.
6. L. Ouyang, E. Steenbergen, O. O. Cellek, Y.-H. Zhang, and D. J. Smith, “Structural properties of InAs/InAs1-xSbx type-II superlattices”, SPIE Photonics West, San Francisco, Jan. 2012.
7. Y.-H. Zhang, “6.1 Å II-VI and III-V materials: A platform for photovoltaic and IR device applications”, The 15th International Conference on II-VI Compounds, Mexico, Aug. 2011.
8. Y.-H. Zhang, “6.1 Å II-VI and III-V materials: A platform for photovoltaic, thermophotovoltaic, and thermoelectric device applications”, Advanced Concepts in Semiconductor Materials and Devices for Energy Conversion, Beltsville, Maryland, December 7-8, 2010.

1.

1. Report Type

Final Report

Primary Contact E-mail

Contact email if there is a problem with the report.

loriann.brichetto@asu.edu

Primary Contact Phone Number

Contact phone number if there is a problem with the report

480-965-8222

Organization / Institution name

Arizona State University

Grant/Contract Title

The full title of the funded effort.

Multicolor (UV-IR) photodetectors based on lattice-matched 6.1 Å II/VI and III/V semiconductors

Grant/Contract Number

AFOSR assigned control number. It must begin with "FA9550" or "F49620" or "FA2386".

FA9550-10-1-0129

Principal Investigator Name

The full name of the principal investigator on the grant or contract.

Yong-Hang Zhang

Program Manager

The AFOSR Program Manager currently assigned to the award

Kenneth Goretta

Reporting Period Start Date

4/1/2012

Reporting Period End Date

5/14/2015

Abstract

This program focused on the demonstration of a novel idea to use optical biasing for multi-color detection using two-terminal monolithically integrated multi-junction photodetectors (MJPDs). Using optical biasing, any sub-photodetector can be selected to limit the current and the multi-color photodetector detects light within the wavelength range of the selected sub-photodetector, namely, optical addressing. This idea has been firstly demonstrated in a monolithic GaInP/Ga(In)As/Ge triple-junction solar cell. Later on, the optical addressing has been achieved in a near-and-long-wave infrared multiband photodetector integrated by a NIR AlGaAs/GaAs PIN sub-photodetector and a LWIR AlGaAs/GaAs n-QWIP sub-photodetector. Finally, the optical addressing has been realized in a visible-and-mid-wave-infrared multi-color photodetector based on II-VI and III-V semiconductors. This photodetector consists of a newly-proposed CdTe/ZnTe/CdTe nBn sub-photodetector for visible light detection and a well-developed InSb PIN sub-photodetector for MWIR detection, which are electrically connected by a perfectly conductive n-CdTe/p-InSb tunnel junction.

Distribution Statement

This is block 12 on the SF298 form.

Distribution A - Approved for Public Release

Explanation for Distribution Statement

If this is not approved for public release, please provide a short explanation. E.g., contains proprietary information.

SF298 Form

Please attach your SF298 form. A blank SF298 can be found here. Please do not password protect or secure the PDF The maximum file size for an SF298 is 50MB.

FA9550-10-1-0129 SF298.pdf

Upload the Report Document. File must be a PDF. Please do not password protect or secure the PDF . The maximum file size for the Report Document is 50MB.

FA9550-10-1-0129 Multicolor project report final.pdf

Upload a Report Document, if any. The maximum file size for the Report Document is 50MB.

Archival Publications (published) during reporting period:

X.-M. Shen, H. Li, S. Liu, D. J. Smith, Y.-H. Zhang, Study of InAs/InAsSb type-II superlattices using high-resolution x-ray diffraction and cross-sectional electron microscopy, J. of Cryst. Growth 381, 1-5 (2013).

2. J. Fan, X. Liu, L. Ouyang, R. E. Pimpinella, M. Dobrowolska, J. K. Furdyna, D. J. Smith, and Y.-H. Zhang, "Molecular beam epitaxial growth of high-reflectivity and broad-bandwidth ZnTe/GaSb distributed Bragg reflectors", J. Vac. Sci. Technol. B 31, 03C109 (2013).

3. J. Fan, L. Ouyang, X. Liu, J. K. Furdyna, D. J. Smith, and Y.-H. Zhang, "GaSb/ZnTe doubleheterostructures grown using molecular beam epitaxy", J. of Crystal Growth 371 (1), 122–125 (2013).

4. S. Liu, H. Li, O. O. Cellek, D. Ding, X.-M. Shen, E. H. Steenbergen, Z.-Y. Lin, J. Fan, Z.-Y. He, J. Lu, S. R. Johnson, D. J. Smith, and Y.-H. Zhang, "Impact of substrate temperature on the structural and optical properties of strain-balanced InAs/InAsSb type-II superlattices grown by molecular beam epitaxy", Appl. Phys. Lett. 102, 071903-071903-4 (2013).

5. H. Li, S. Liu, O. O. Cellek, D. Ding, X.-M. Shen, E. H. Steenbergen, J. Fan, Z. Lin, Z.-Y. He, Q. Zhang, P. T. Webster, S. R. Johnson, L. Ouyang, D.J. Smith, and Y.-H. Zhang, "A calibration method for group V fluxes and impact of V/III flux ratio on the growth of InAs/InAsSb type-II superlattices by molecular beam epitaxy", J. of Crystal Growth 378, 145-149 (2013).

6. H.S. Kim, O.O. Cellek, Z. Lin, Z.-Y. He, H. Li, S. Liu, and Y.-H. Zhang, "Long-wave infrared nBn photodetectors based on InAs/InAsSb type-II superlattices", Applied Physics Letters 101, 161114 (2012).

7. O.O. Cellek, J.L. Reno, Y.-H. Zhang, "Optically addressed near and long-wave infrared multiband photodetectors", Applied Physics Letters 100, 241103-41103. (2012)

8. X. Liu, D. J. Smith, H. Cao, Y. P. Chen, J. Fan, Y.-H. Zhang, R. E. Pimpinella, M. Dobrowolska, and J. K. Furdyna, "Characterizations of Bi2Te3 and Bi2Se3 topological insulators grown by MBE on (100) GaAs substrates", J. Vac. Sci. Technol. B 30, 02B103 (2012).

9. M. J. DiNezza, Q. Zhang, D. Ding, J. Fan, X. Liu, J. K. Furdyna, Y.-H. Zhang, "Aluminum diffusion in ZnTe films grown on GaSb substrates for n-type doping", physica status solidi (c), 9, 1720–1723 (2012).

10. Q. Zhang, X. Liu, M. J. DiNezza, J. Fan, D. Ding, J. K. Furdyna, Y.-H. Zhang, "Influence of Te/Zn flux ratio on Aluminum doped ZnTe grown by MBE on GaSb substrates", physica status solidi (c), 9, 1724–1727 (2012).

11. E. H. Steenbergen, K. Nunna, L. Ouyang, B. Ullrich, D. L. Huffaker, Y.-H. Zhang, "Strainbalanced InAs/InAs1-xSbx type-II superlattices grown by molecular beam epitaxy on GaSb substrates", J. Vac. Sci. Technol. B 30, 02B107 (2012).

12. J. Fan, L. Ouyang, X. Liu, D. Ding, J. K. Furdyna, D. J. Smith, and Y.-H. Zhang, “Influence of temperature ramp on the materials properties of GaSb grown on ZnTe using molecular beam epitaxy”, J. Vac. Sci. Technol. B, 30, 02B122 (2012).

13. E. H. Steenbergen, B. C. Connelly, G. D. Metcalfe, H. Shen, M. Wraback, D. Lubyshev, Y. Qiu, J. M. Fastenau, A. W. K. Liu, S. Elhamri, O. O. Cellek, and Y.-H. Zhang, “Significantly improved minority carrier lifetime observed in a long-wavelength infrared III-V type-II superlattice comprised of InAs/InAsSb”, Appl. Phys. Lett. 99, 251110 (2011).

14. X. Liu, D. J. Smith, J. Fan, Y.-H. Zhang, H. Cao, Y. P. Chen, J. Leiner, B. J. Kirby, M. Dobrowolska, and J. K. Furdyna, “Structural properties of Bi2Te3 and Bi2Se3 topological insulators grown by molecular beam epitaxy on GaAs(100) substrates”, Appl. Phys. Lett. 99, 171903 (2011).

15. E. H. Steenbergen, Y. Huang, J.-H. Ryou, L. Ouyang, J.-J. Li, D. J. Smith, R. D. Dupuis, Y.-H. Zhang, “Structural and optical characterization of type-II InAs/InAs1-xSbx superlattices grown by metalorganic chemical vapor deposition”, Appl. Phys. Lett. 99, 071111 – 071114 (2011).

16. E. H. Steenbergen, M. J. DiNezza, W. H. G. Dettlaff, S. H. Lim, Y.-H. Zhang, “Effects of varying light bias on an optically-addressed two-terminal multi-color photodetector”, Infrared Physics and Technology 54, 292-295 (2011).

17. Y. Huang, J.-H. Ryou, R. D. Dupuis, V. R. D’Costa, E. H. Steenbergen, J. Fan, Y.-H. Zhang, A. Petschke, M. Mandl, S.-L. Chuang, “Epitaxial growth and characterization of InAs/GaSb and InAs/InAsSb type-II superlattices on GaSb substrates by metalorganic chemical vapor deposition for long wavelength infrared photodetectors”, J. of Cryst. Growth 314, 92-96 (2011).

18. J. Fan, L. Ouyang, X. Liu, D. Ding, J.K. Furdyna, D. J. Smith and Y.-H. Zhang, “Growth and material properties of ZnTe on GaAs, InP, InAs and GaSb (0 0 1) substrates for electronic and optoelectronic device applications”, J. of Cryst. Growth 323, 127-131 (2010).

19. E. H. Steenbergen, M. J. DiNezza, W. H. G. Dettlaff, S. H. Lim, Y.-H. Zhang, “Opticallyaddressed two-terminal multi-color photodetector”, Appl. Phys. Lett. 97 161111-161114 (2010).

Changes in research objectives (if any):

Change in AFOSR Program Manager, if any:

Extensions granted or milestones slipped, if any:

AFOSR LRIR Number

LRIR Title

Reporting Period

Laboratory Task Manager

Program Officer

Research Objectives

Technical Summary

Funding Summary by Cost Category (by FY, $K)

	Starting FY	FY+1	FY+2
Salary			
Equipment/Facilities			
Supplies			
Total			

Report Document

Report Document - Text Analysis

Report Document - Text Analysis

Appendix Documents

2. Thank You

E-mail user

Aug 24, 2015 18:56:57 Success: Email Sent to: loriann.brichetto@asu.edu